Moreno-Rodriguez *et al.*
Journal of Neuroinflammation (2025) 22:25
https://doi.org/10.1186/s12974-025-03349-y

Journal of Neuroinflammation

RESEARCH **Open Access**

APOEε4 alters ApoE and Fabp7 in frontal cortex white matter in prodromal Alzheimer's disease

Marta Moreno-Rodriguez[1], Sylvia E. Perez[1], Michael Malek-Ahmadi[2] and Elliott J. Mufson[1,3*]

Abstract
The ApoE ε4 allele (APOEε4) is a major genetic risk factor for sporadic Alzheimer's disease (AD) and is linked to demyelination and cognitive decline. However, its effects on the lipid transporters apolipoprotein E (ApoE) and fatty acid-binding protein 7 (Fabp7), which are crucial for the maintenance of myelin in white matter (WM) during the progression of AD remain underexplored. To evaluate the effects of APOEε4 on ApoE, Fabp7 and myelin in the WM of the frontal cortex (FC), we examined individuals carrying one ε4 allele that came to autopsy with a premortem clinical diagnosis of no cognitive impairment (NCI), mild cognitive impairment (MCI) and mild to moderate AD compared with non-carrier counterparts. ApoE, Fabp7 and Olig2 immunostaining was used to visualize cells, whereas myelin basic protein (MBP) immunocytochemistry and luxol fast blue (LFB) histochemistry of myelin in the WM of the FC were combined with quantitative morphometry. We observed increased numbers of ApoE-positive astrocytes in the WM of both NCI and MCI APOEε4 carriers compared with non-carriers, whereas Fabp7-positive cells were elevated only in AD. Conversely, Olig2 cell counts and MBP immunostaining decreased in MCI APOEε4 carriers compared to non-carriers, while LFB levels were higher in NCI APOEε4 carriers compared to non-carriers. Although no correlations were found between ApoE, Fabp7, and cognitive status, LFB measurements were positively correlated with perceptual speed, global cognition, and visuospatial scores in APOEε4 carriers across clinical groups. The present findings suggest that the ε4 allele compromises FC myelin homeostasis by disrupting the lipid transporters ApoE, Fabp7 and myelination early in the onset of AD. These data support targeting cellular components related to WM integrity as possible treatments for AD.

Keywords APOEε4, Fabp7, Astrocytes, White matter, Alzheimer's disease, Mild cognitive impairment

Background

The apolipoprotein E ε4 allele (APOEε4) is the most significant genetic risk factor for Alzheimer's disease (AD) and is correlated with a dose-dependent increase in disease onset and cognitive decline [1–4]. Individuals carrying a single ApoE ε4 allele have a three-to-four-fold increase while those with two alleles have an eight to 12-fold increase in the risk of AD compared to one ε4 allele and individuals heterozygous for APOEε4 may represent a distinct genetic subtype of AD [5]. The APOE gene encodes the ApoE protein, a 34 kDa lipidic transporter, comprising 299 amino acid residues that exist in 3 polymorphic alleles: ε2, ε3, and ε4 resulting in six genotypes (APOEε2ε2, ε2ε3, ε3ε3, ε2ε4, ε3ε4, and ε4ε4). The effects of ApoE isoforms, despite their variation of only two amino acid residues at positions 112 and 158

*Correspondence:
Elliott J. Mufson
elliott.mufson@barrowneuro.org
[1] Department of Translational Neuroscience, Barrow Neurological Institute, Phoenix, AZ 85013, USA
[2] Banner Alzheimer's Institute, Phoenix, AZ 85006, USA
[3] Departments of Translational Neuroscience and Neurology, Barrow Neurological Institute, Phoenix, AZ 85013, USA

(APOEε2: Cys112/Cys158; APOEε3: Cys112/Arg158; APOEε4: Arg112/Arg158) [6] on the pathogenesis of AD remain under investigated. The frequency and effect of ApoE alleles vary with age and ethnicity [1–4]. In this regard, the APOEε3 allele is more common than the ε2 allele in Caucasian populations and the latter has been described as a protective genetic factor for AD [7, 8]. The ε4 allele is associated with approximately 65–75% of sporadic AD [9, 10], resulting in different effects between AD APOEε4 carriers [11, 12]. Structural magnetic resonance imaging (MRI) demonstrated that individuals carrying the APOEε4 allele exhibit accelerated hippocampal volume loss in early life and accelerated cortical atrophy during midlife [13]. Positron emission tomography (PET) imaging revealed that APOEε4 correlated with increased amyloid-β (Aβ) deposition rates and the widespread cortical accumulation of Aβ in patients with AD [14]. However, APOEε4 does not affect APP processing in humanized ApoE targeted-replacement mice [15]. APOEε4 accelerates the breakdown of the blood–brain barrier, which is associated with reactive gliosis independent of Aβ pathology in animal models of AD [16, 17]. Despite the influence of APOEε4 on various neuropathological features of AD, its effect on white matter (WM) integrity in those carrying the ε4 allele during the clinical onset of AD remains a significant knowledge gap [11].

ApoE protein is secreted by astrocytes and less so by microglia, oligodendrocytes, and neurons under stress [18–22]. In WM, ApoE is lipidated to meet the lipid demands of oligodendrocytes, including cholesterol, phospholipids, sphingolipids, and glucosylceramides, which are essential for assembling and maintaining the multilayered membrane of the myelin sheath. These lipids act through lipidation, which occurs either within oligodendrocytes or via transport from astrocytes [18, 23, 24]. During aging, oligodendrocytes become less capable of synthesizing fatty acids (FAs) and lipids, leading to an increase in lipid transport from astrocytes to maintain myelin integrity, which are more vulnerable during pathological conditions [23, 25, 26]. Age-related decline in regeneration hinders myelin debris clearance, causing inflammation and impaired remyelination, which can be restored by stimulating cholesterol transport [27]. In the aging rodent brain single-cell RNA sequencing from white and/or grey matter revealed white matter-associated microglia (WAMs), which contain components of the genetic signature for disease-associated microglia (DAM) consisting of the activation of genes implicated in phagocytic activity and lipid metabolism [28]. In aged mice, WAMs appear to be produced in an APOE-independent pathway, whereas the generation of microglia expressing DAM and WAM expression signatures require APOE function in rodent AD models suggesting that differences in brain environment affect the genetics of microglia.

Recent findings suggest that glial fatty acid binding protein 7 (Fabp7), a myelin-fatty acid (FA) related transporter involved in the uptake, transport, metabolism, and storage of fatty acids, is primarily expressed in astrocytes, but also plays a key role in myelin lipid synthesis in the developing and mature brain [29]. Fabp7, the major isoform expressed in oligodendrocyte progenitor cells (OPCs) is upregulated in gray matter astrocytes surrounding Aβ plaques, suggesting a neuroinflammatory role in AD [30–32]. Interestingly, myelin loss together with oligodendrocyte impairment occurs decades prior to the onset of cognitive symptoms or the presence of Aβ and tau lesions in AD [33–35]. Diffusion tensor imaging has revealed microstructural damage to WM in healthy adults carrying the APOEε4 allele [36–39], which disrupts cholesterol binding leading to aberrant deposition of oligodendrocytes and reduced myelination compared to APOEε4 non-carriers, due to decreased lipid transport between these cells [7, 40]. There is also a loss of oligodendrocytes in the FC of APOEε4 carriers compared to non-carriers in sporadic and familial AD [41] suggesting that APOEε4 disrupts myelin homeostasis highlighting the importance of myelin-preserving proteins including lipid transporters during the onset of AD. Therefore, lipid transporters, ApoE and Fabp7, likely play a major role in the assembly and maintenance of myelin during aging and pathological disorders [42, 43].

The present study evaluated the cellular expression of the lipid transporters ApoE and Fabp7 as well as myelin within the WM of FC in heterozygous APOEε4 carriers compared with non-carriers who at time of death received a premortem clinical diagnoses of no cognitive impairment (NCI), mild cognitive impairment (MCI) and mild to moderate AD. This approach differs from other studies that base AD progression upon Braak tau staging scores [41], which have shown inconsistent correlations with clinical stages of dementia [44, 45]. Currently, no studies have examined lipid protein alterations in the WM in the prodromal stage of AD. Understanding the mechanisms by which myelin maintenance is compromised in APOEε4 carriers could reveal novel biomarkers and therapeutic interventions for AD.

Materials and methods

Subjects

In this study, individuals were randomly selected on the basis of the last premortem clinical diagnosis of no cognitive impairment (NCI, n = 26), mild cognitive impairment (MCI, n = 22), and mild to moderate AD (AD, n = 22) from participants of the Rush Religious

Orders Study (RROS) cohort as part of our ongoing NIA funded program project grant (PO1AG014449). Cases selection was not based upon postmortem Braak stage, which can range from stage II-V within cases with a premortem clinical diagnosis of NCI, MCI and AD from the RROS [44–46] and other clinical cohorts [47, 48]. We divided each clinical group by genotype; (APOEε3ε3) APOEε4 non-carriers (Table 1) and (APOEε3ε4) APOEε4 carriers (Table 2). The Human Research Committees of Rush University Medical Center and Dignity Health approved this study and written informed consent for research and brain

Table 1 Demographic, cognitive, and neuropathological data by clinical group for APOEε4 non-carriers

	NCI (n = 15)	MCI (n = 12)	AD (n = 11)	P-value	Groupwise comparison
Age at death	86.43 ± 5.81	88.42 ± 4.79	91.40 ± 2.65	0.06	Na
	[78, 95]	[79, 96]	[87, 95]		
Education	18.39 ± 4.38	17.68 ± 3.60	17.27 ± 3.55	0.77	Na
	[10, 27]	[10, 20]	[9, 21]		
Sex (M/F)	9/6	4/8	3/8	0.19	Na
MMSE	28.19 ± 1.36	26.17 ± 2.80	16.45 ± 7.23	0.003	NCI > MCI > AD
	[25, 30]	[19, 30]	[2, 27]		
GCS	0.11 ± 0.36	−0.50 ± 0.42	−1.40 ± 0.81	< 0.001	NCI > AD
	[−0.54, 0.87]	[−0.95, 0.40]	[−2.56, 0.08]		
Episodic memory	0.45 ± 0.48	−0.45 ± 0.79	−1.60 ± 1.37	< 0.001	NCI > AD
	[−0.40, 1.30]	[−1.46, 1.31]	[−3.69, 0.67]		
Semantic memory	0.02 ± 0.56	−0.25 ± 0.47	−1.06 ± 0.77	0.01	NCI > AD
	[−1.44, 0.77]	[−1.13, 0.47]	[−2.39, 0.07]		
Working memory	−0.07 ± 0.66	−0.51 ± 0.46	−1.08 ± 1.07	0.07	Na
	[−1.01, 0.55]	[−1.03, 0.39]	[−2.77, 0.57]		
Perceptual speed	−0.42 ± 0.64	−1.02 ± 0.75	−1.96 ± 0.86	0.001	NCI > AD
	[−1.63, 0.87]	[−2.28, 0.24]	[−3.38, −0.64]		
Visuospatial	0.05 ± 0.67	−0.56 ± 0.77	−0.69 ± 0.60	0.09	Na
	[−1.00, 1.78]	[−2.42, 0.44]	[−1.56, 0.30]		
Post-morteminterval	5.91 ± 1.42	5.83 ± 2.33	4.55 ± 1.47	0.12	Na
	[3, 8]	[2, 11]	[2, 7]		
Brain weight at autopsy	1,169.47 ± 159.33	1,185.92 ± 138.45	1,100.30 ± 83.29	0.32	Na
	[943, 1488]	[990, 1480]	[950, 1245]		
Braak stage				0.15	Na
0-II	4	2	2		
III-IV	10	9	4		
V-VI	1	1	5		
CERAD				0.27	Na
No AD	2	3	1		
Possible AD	2	2	1		
Probable AD	9	5	3		
Definite AD	2	2	6		
NIA reagan diagnosis				0.09	Na
Not AD	0	0	0		
Low likelihood	2	5	2		
Intermediate likelihood	5	6	5		
High likelihood	4	1	4		
A score	3 [0–3]	3 [2–5]	3 [0–5]		
B score	2 [1–3]	2 [1–3]	2 [1–3]		
C score	2 [0–3]	2 [0–3]	3 [0–3]		
TDP-43	0 [0–1]	0 [0–1]	2 [0–3]		

Table 2 Demographic, cognitive, and neuropathological data by clinical group for APOEε4 Carriers

	NCI (n = 11)	MCI (n = 10)	AD (n = 11)	P-value	Groupwise comparison
Age at death	85.60 ± 6.66	88.35 ± 5.32	87.14 ± 5.89	0.70	Na
	[70, 93]	[79, 98]	[76, 87]		
Education	19.45 ± 3.14	19.10 ± 3.81	19.27 ± 3.90	0.95	Na
	[14, 24]	[12, 25]	[12, 26]		
Sex (M/F)	6/5	5/5	3/8	0.39	Na
MMSE	28.09 ± 0.94	26.50 ± 2.32	18.36 ± 6.77	< 0.001	NCI > MCI > AD
	[27, 30]	[12, 25]	[4, 28]		
GCS	0.30 ± 0.24	−0.56 ± 0.47	−1.86 ± 0.76	< 0.001	NCI > MCI, AD
	[−0.07, 0.76]	[−1.56, 0.02]	[−3.49, −0.95]		
Episodic memory	0.58 ± 0.42	−0.69 ± 0.82	−2.25 ± 1.00	< 0.001	NCI > MCI, AD
	[−0.01, 1.31]	[−2.70, 0.18]	[−3.91, −0.88]		
Semantic memory	0.21 ± 0.36	−0.23 ± 0.46	−1.54 ± 1.13	< 0.001	NCI > AD
	[−0.23, 1.02]	[−1.21, 0.36]	[−3.91, −0.10]		
Working memory	0.24 ± 0.79	−0.48 ± 0.51	−1.17 ± 0.85	0.001	NCI > AD
	[−0.89, 1.78]	[−1.25, −0.23]	[−3.23, −0.09]		
Perceptual speed	−0.34 ± 0.57	−1.08 ± 0.68	−2.10 ± 0.81	< 0.001	NCI > AD
	[−1.11, 0.77]	[−2.46, −0.04]	[−2.96, −0.54]		
Visuospatial	0.29 ± 0.50	−0.25 ± 0.52	−1.32 ± 0.52	< 0.001	NCI, MCI > AD
	[−0.32, 1.02]	[−0.98, 0.86]	[−2.58, −0.86]		
Post-mortem interval	10.99 ± 5.98	6.62 ± 5.72	5.54 ± 2.25	0.05	Na
	[3, 20]	[1, 20]	[1.50, 8.17]		
Brain weight at autopsy	1,262.45 ± 141.41	1,218.00 ± 165.04	1,198.18 ± 157.52	0.58	Na
	[963, 1460]	[890, 1450]	[1044, 1460]		
Braak stage				0.16	Na
0-II	3	1	1		
III-IV	8	5	3		
V-VI	0	4	8		
CERAD				0.64	Na
No AD	2	2	2		
Possible AD	3	2	0		
Probable AD	3	4	4		
Definite AD	3	2	5		
NIA reagan diagnosis				0.06	Na
Not AD	0	0	2		
Low likelihood	4	5	1		
Intermediate likelihood	7	3	4		
High likelihood	0	2	4		
A score	4 [0–5]	4 [3–5]	4 [3–5]		
B score	2 [0–2]	2 [1–3]	3 [1–3]		
C score	2 [0–3]	2 [0–3]	3 [2, 3]		
TDP-43	0 [0–3]	0 [0–3]	2 [0–3]		

autopsy was obtained from the participants or their family/guardians.

Clinical and neuropathological evaluation

Tables 1 and 2 show the demographic, clinical and neuropathological characteristics of the cases examined. The clinical and neuropathological criteria for NCI, MCI, and AD were reported previously [21, 49–52]. Briefly, after a review of the clinical data and examination of the participants, clinical diagnoses were made by a board-certified neurologist with expertise in gerontology. The neurologist reviewed the medical history, medication use, neurologic examination information, results of cognitive performance testing, and the neuropsychologist's opinion of cognitive impairment and the presence of dementia. Each participant was evaluated in his/her home, emphasizing clinically relevant findings. The AD diagnosis of dementia followed the recommendations of the joint working group of the National Institute of Neurological and Communicative Disorders and the Stroke and the Alzheimer's disease and Related Disorders Association (NINCDS/ADRDA) [53]. The clinical classification of mild cognitive impairment, used in the present study is compatible with that used by many others in the field to describe those persons who are not cognitively normal, but do not meet the accepted criteria for dementia [54–59]. Here, MCI was defined as a person rated as impaired on neuropsychological testing by the neuropsychologist but who was not found to have dementia by the examining neurologist. The average time from the last clinical evaluation to death was ~ 8 months. Clinical neuropsychological tests included the Mini-Mental State Examination, global cognitive score, composite z-score compiled from 19 cognitive tests, and z-scores from episodic memory, semantic memory, working memory, perceptual speed, and visuospatial tests. Postmortem neuropathology was performed as reported previously [49, 50, 52, 60], which included Braak staging [61], NIA-Reagan criteria [62], and the Consortium to Establish a Registry for Alzheimer's disease (CERAD) [63]. These cases were also evaluated for transactive response DNA-binding protein 43 kDa (TDP-43) inclusions [64] and assigned ABC criteria [54]. A board-certified neuropathologist excluded cases with other pathologies (e.g., cerebral amyloid angiopathy, vascular dementia, dementia with Lewy bodies, hippocampal sclerosis, Parkinson's disease, large strokes, and individuals treated with acetylcholinesterase inhibitors).

Immunohistochemistry

Two 8-µm-thick paraffin-embedded FC (Brodmann's area 10, BA10) sections were processed for immunocytochemistry. Sections were pretreated with either citric acid (pH = 6) for 10 min for antigen retrieval for APOE (Goat anti-APOE, [1:6000], Ab947, Millipore), MBP (Rat anti-MBP, [1:500], Ab7349, Abcam), Fabp7 (Rabbit anti-Fap7, [1:500], PA5-24949, Thermo Fisher Scientific), AT8 (mouse anti-Phospho-Tau (Ser202, Thr205), [1:100], Thermo Fisher Scientific). Antigen retrieval consisting of 80% formic acid for 15 min following citric acid treatment was performed prior to Olig2 antibody [Rabbit anti-Olig2 (1:100), Ab109186, Abcam] incubation, whereas tissue was only pretreated with 80% formic acid for 10 min prior to treatment with the 6E10 antigen (Mouse anti-beta-Amyloid 1–16, [1:500], 803002, BioLegend). Sections were then incubated over night with primary antibodies at room temperature (RT) in a tris-buffered saline (TBS)/0.25% Triton X-100/1% goat serum solution. After several washes in TBS, tissues were incubated for 1 h with a goat anti-rabbit/anti-rat biotinylated secondary antibody, incubated in Vectastain ABC kit (1 h) (Vector Labs, Burlingame, CA) and developed in a solution consisting of acetate-imidazole buffer containing 0.05% 3,3′-diaminobenzidine tetrahydrochloride (DAB, Sigma, MO). Immunocytochemical controls consisted of the omission of the primary antibody, which resulted in an absence of immunoreactivity [65]. The specificity of the ApoE antibody was determined by western blot (WB), which reacts with the ApoE isoforms E2, E3, and E4 (RRID: AB_2258475) according to the manufacturer's instructions. The MBP antibody was generated against a recombinant fragment of amino acids 82–87 (DENPVV) (RRID: AB 305869) by the manufacturer. Fabp7 was raised against a KLH-conjugated synthetic peptide spanning amino acids 104–132 from the C-terminal region of human Fabp7. Antibody specificity for Olig2 (RRID: AB_10861310) and Fabp7 (RRID: AB_2542449) was reported by the manufacturer. The 6E10 antibody is a purified anti-Aβ mouse monoclonal antibody (1–16) raised against the epitope within amino acids 3–8 of human Aβ (BioLegend, 803003; RRID: AB_2564652). The anti-phospho-tau mouse monoclonal (Invitrogen, MN1020, RRID: AB_223647, clone AT8) recognizes the phosphatase epitope Ser202/Thr205 of PHF-tau. The manufacturer reported the antibody specificity for these last two antibodies. The variability in the number of cases per experiment is due to limited tissue availability for some of the samples.

Immunofluorescence

Eight-µm-thick paraffin-embedded FC sections were deparaffinized and pretreated with either citric acid (pH = 6) for 10 min followed by treatment with 80% formic acid for 15 min for ApoE, GFAP and Fabp7 for antigen retrieval. Sections were double or triple labeled with either a rabbit anti-GFAP (Z0334, Dako, RRID:AB_10013382), 1:500 dilution or a mouse anti-GFAP [1:50 dilution] monoclonal antibody, unconjugated, clone GA5, 3670S (Cell Signaling Technology, RRID:AB_561049), Iba1 (Rabbit anti-Iba1 [1:50], 019–19741, FUJIFILM Wako Pure Chemical Corporation, RRID:AB_839504), Fabp7 (Rabbit anti-Fap7 [1:50], PA5-24949, Thermo Fisher Scientific, RRID:AB_2542449) or Olig2 (Rabbit anti-Olig2 [1:50], AB109186, Abcam, RRID:AB_10861310) together with an ApoE (Goat anti-ApoE [1:500], Ab947, Millipore, RRID:AB_305869) antibody overnight. The appropriate secondary antibodies were applied (Cy2-donkey anti-mouse IgG for GFAP, Cy3-donkey anti-goat IgG for ApoE and Cy5-donkey anti-rabbit IgG for Fabp7, Iba1, GFAP and Olig2 [1:200], Jackson Immuno-research). Autofluorescence was blocked with autofluorescence Eliminator Reagent (Millipore, Burlington, MA) and sections were cover-slipped with aqueous mounting media (Thermo Scientific). Dual and triple immunofluorescence were visualized and images were acquired using a Revolve Fluorescent Microscope (Echo Laboratories, San Diego, CA, USA) with excitation filters 405 for Cy2 (emission green; pseudocolored red) and 489 for Cy3 (emission red; pseudocolored blue) [65]. Immunofluorescent controls consisted of the omission of each primary antibody, which resulted in an absence of immunoreactivity.

Luxol fast blue histochemistry

Eight-µm-thick paraffin-embedded FC sections were washed in absolute ethanol for 5 min, incubated in a solution containing luxol fast blue (LFB) dissolved in 95% ethanol at 60 °C overnight, rinsed in 70% ethanol followed by distilled water and differentiated in a 0.05% Li_2CO_3 solution for 30 s. Sections were transferred into 70% ethanol, rinsed in distilled water and cover-slipped using DPX (Electron Microscopy Sciences, Hatfield, PA).

Quantitation of ApoE, Fabp7, Olig2-positive cells and phosphorylated AT8 positive cells and 6E10 positive plaques

We marked 10 WM regions of interest (ROIs) per slide at 1X magnification from two FC sections from both APOEε4 non-carriers and APOEε4 carriers in cases with a premortem clinical diagnosis of NCI, MCI, and AD and counted ApoE, Fabp7, and Olig2-positive cells. For AT8 positive cells or 6E10 labeled plaques we marked 5 ROIs per slide. Directly below each marked ROI we counted ApoE, Fabp7, and Olig2-positive cells within the WM and AT8 positive cells or 6E10 positive plaques within both GM and WM at 40×magnification before moving to the next area avoiding overlapping regions. All images and counts were performed using a Nikon Eclipse 80i coupled with NIS-Elements Imaging software (Nikon Americas Inc., NY). Counts stratified by clinical group and APOEε4 status are shown in Table S1 [65]. Counts were performed by an investigator blinded to clinical, pathological and genotype to ensure unbiased analysis.

Quantification of white matter MBP, LFB, and cellular ApoE optical density values

We performed optical density (OD) measurements of cellular ApoE, MBP immunoreactivity and LFB histochemistry in 10 selected ROIs within a 0.14 mm^2 area of WM in two FC sections from NCI, MCI, and AD APOEε4 non-carriers and APOEε4 carriers. Densitometry measurements of MBP and LFB labeling were performed within the entire ROI. Each OD value was automatically analyzed in grayscale and background OD values were subtracted from the measurements of MBP, LFB, and ApoE. All images and OD values were performed with the aid of a Nikon Eclipse 80i coupled with NIS-Elements Imaging software (Nikon Americas Inc., NY). OD values stratified by clinical group and APOEε4 status are shown in Table S1 [65]. ApoE-positive cells within a ROI were manually outlined at 40X magnification. OD measurements were also performed blinded to clinical, pathological and genotype to ensure unbiased analysis.

Statistical analysis

Analysis across clinical groups Šidákwas performed using the Mann–Whitney, Kruskal–Wallis, chi–square, and Wilcoxon signed–rank tests followed by Conover–Inman, Holm–Šidák, Tukey and Dunn's post hoc tests for multiple comparisons and Spearman rank for correlations. A false discovery rate was used to adjust for multiple comparisons between correlations. Linear regression models were used to evaluate the association between independent variables (APOEε4 carrier status, ApoE, Olig 2 and Fabp7 cell counts) and the dependent variables (LFB and MBP ODs). Statistical significance was set at $p < 0.05$ (two-tailed) and the data were graphically represented with aid of GraphPad Prism 9 (GraphPad Software, San Diego, CA, USA).

Results

Subject characteristics

Demographic, clinical, and neuropathological characteristics of the 70 cases are summarized in Table 1 (APOEε4 non-carriers) and Table 2 (APOEε4 carriers). There were no significant differences in age, years of education, sex, postmortem interval (PMI), brain weight, Braak scores, CERAD, NIA Reagan diagnosis independent of genotype. The NIA-AA ABC scores and the percentage of cases displaying pathological TDP-43 were similar between clinical groups in both genotypes (Tables 1 and 2). The similarity of the deposition of Aβ seen in the NCI and MCI cases, suggests that the former were presumably in the progression to AD. MMSE was significantly lower in AD compared to both NCI and MCI groups in both genotypes (Kruskal–Wallis followed by a Dunn's test: NCI > MCI > AD, $p = 0.003$ APOEε4 non-carriers and $p < 0.001$ APOEε4 carriers). Semantic memory and perceptual speed scores were reduced in AD compared to NCI independent of genotype (Kruskal–Wallis followed by a Dunn's test: NCI > AD, $p \leq 0.001$). Working memory and visuospatial scores were comparable across clinical groups in APOEε4 carriers but significantly lower in AD compared to NCI in APOEε4 non-carriers

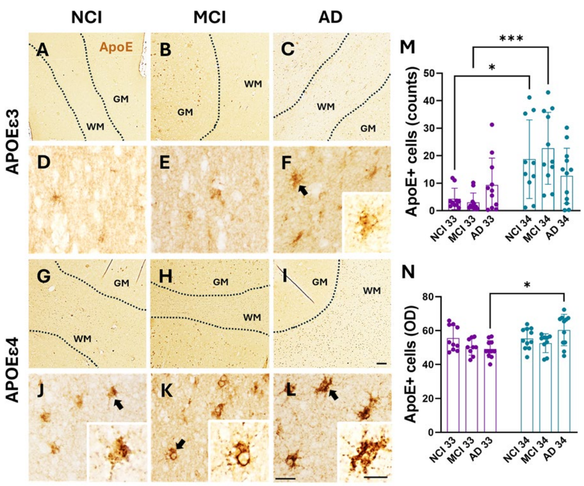

Fig. 1 FC WM ApoE positive cells in NCI, MCI, and AD APOEε4 carriers and non-carriers. Low magnification images of ApoE reactivity in the WM (dashed lines) of APOEε3 (**A**–**C**) and APOEε4 (**G**–**I**) carriers. Higher magnification images of ApoE positive cells in WM displaying an astrocyte phenotype in the APOEε3 (**D**–**F**) and APOEε4 (**J**–**L**) groups. Statistical analysis revealed a significant increase in the number (**M**) of ApoE positive cells in NCI and MCI APOEε4 carriers compared with non-carriers and in OD ApoE values (**N**) in AD APOEε4 carriers compared with non-carriers (NCI3/3 n = 10, MCI3/3 n = 11, AD3/3 n = 11, NCI3/4 n = 11, MCI3/4 n = 11, AD3/4 n = 12). Boxed insects show high magnification images of ApoE positive cells (arrows). Scale bar in I = 250 µm and applies to panels A-C, G-I. Scale bar in L = 25 µm and inset = 10 µm applies to panels (**D**–**F**, **J**–**L**). Data shown in scatter plot and bar graphs are presented as mean ± SEM. Statistical significance was determined using the Kruskal–Wallis followed by a Dunn's test for comparisons across clinical groups and Mann–Whitney test for comparisons between carriers and non-carriers within each clinical group. Significance levels (*) were set at: *$p < 0.05$, **$p < 0.01$, ***$p < 0.001$. *GM* grey matter, *WM* white matter

(Kruskal–Wallis followed by a Dunn's test: NCI > AD, $p \leq 0.001$ APOEε4 carriers). Global cognition and episodic memory scores were significantly lower in AD compared to NCI APOEε4 non-carriers but were lower in MCI compared to NCI APOEε4 carriers (Kruskal–Wallis followed by a Dunn's test: NCI > AD, $p \leq 0.001$ APOEε4 non-carriers, NCI > MCI, AD $p \leq 0.001$ APOEε4 carriers). Finally, age of death for APOEε4 carriers was significantly lower than APOEε4 non-carriers in the AD cohort (Mann–Whitney test: NCI 3/3 > NCI 3/4, $p = 0.03$).

FC ApoE-immunostaining in APOEε4 non-carriers and carriers during disease progression

ApoE-immunolabeled cells in the WM displayed a star-shaped morphology with numerous ramified processes extending outwardly characteristic of astrocytes across clinical groups. In the WM, we observed a few lightly labeled ApoE-positive cells in NCI and MCI APOEε4 non-carriers (Fig. 1A, B, D, E). Although there was a trend toward an increase in ApoE-positive cells in AD compared with NCI and MCI within APOEε4 non-carriers (Fig. 1C, F), statistical analysis showed no significant differences (Fig. 1J). In the APOEε4 carriers, ApoE labeled cells displayed greater immunoreactive, size, number, and extent of processes (Fig. 1G–L) across clinical groups compared to APOEε4 non-carriers. Quantitation revealed significantly greater numbers of ApoE-positive cells in NCI and MCI APOEε4 carriers compared to non-carriers (Fig. 1J) (Mann–Whitney test: NCI3/3 < NCI3/4, $p = 0.01$, MCI3/3 < MCI3/4, $p < 0.0001$). Although the number of ApoE-positive cells was similar between AD APOEε4 carriers and non-carriers, OD values of ApoE immunostaining were significantly greater in APOEε4 carriers (Fig. 1K) (Mann–Whitney test: AD3/3 < AD3/4, $p = 0.01$).

FC Fabp7-immunostaining in APOEε4 non-carriers and carriers during disease progression

Fabp7-positive cells were small, rounded, or oval shaped with thin often elongated branches displaying a 'spidery' appearance with multiple fine extensions extending in various directions, resembling oligodendrocyte precursor cells (OPCs) [29] (Fig. 2A–L). The number of Fabp7-positive cells decreased significantly in the WM of AD compared to NCI APOEε4 non-carriers (Table S1, Kruskal–Wallis followed by a Dunn's test: NCI3/3 > AD3/3, $p = 0.017$) (Fig. 2A–F, M). By contrast, there was no difference in cell number of APOEε4 carriers across clinical groups. A between genotype analysis of AD APOEε4 carriers revealed a significantly greater number of Fabp7-positive cells compared to non-carriers (Fig. 2F, L, M. Table S1, Mann–Whitney test: AD3/3 < AD3/4, $p = 0.02$).

Fabp7 and ApoE dual labeling in FC white matter of APOEε4 non-carriers and carriers with AD

Immunostaining showed that ApoE-positive cells exhibited an astrocytic phenotype in 85% of the cases examined. However, we observed variability in the phenotype of ApoE-positive cells in the remaining 15% of cases. In contrast, all Fabp7-positive cells revealed exhibited a phenotype distinct from astrocytes. To identify these cells more accurately, we performed triple and double staining of ApoE and Fabp7 with glial markers in selected samples.

To identify these cells more accurately, we performed triple and double staining of ApoE and Fabp7 with glial markers in selected samples. ApoE-positive astrocytes were co-labeled with glial fibrillary acidic protein (GFAP) confirming an astrocytic phenotype (Fig. 3A, B, G, H) in 85% of the cases. ApoE positive but GFAP-negative cells

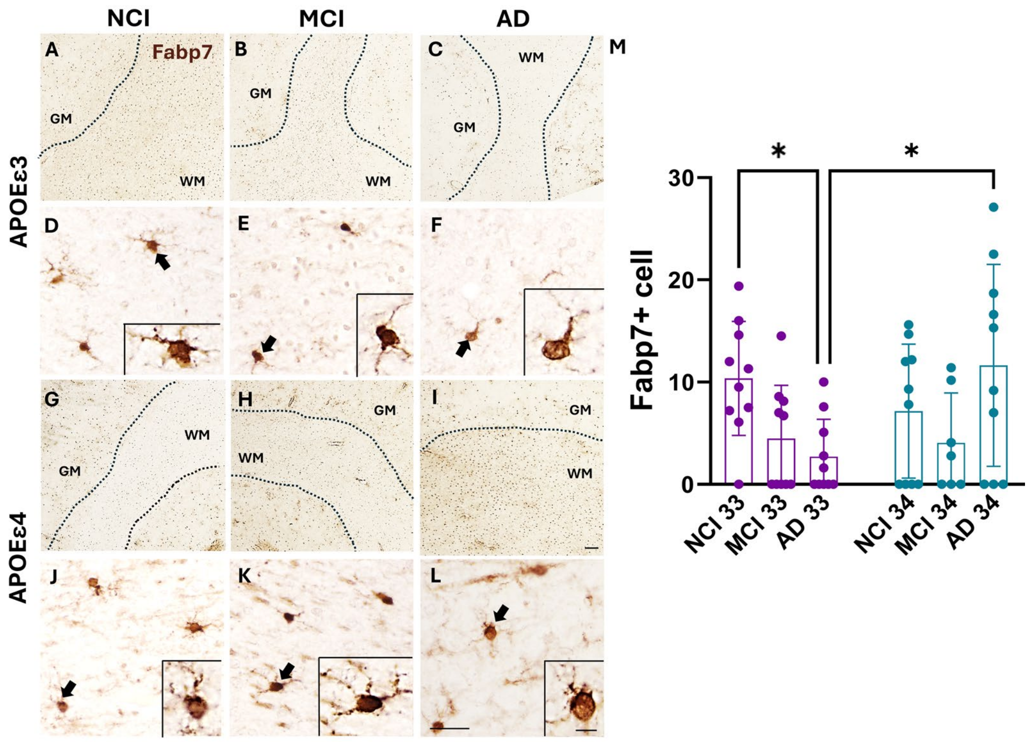

Fig. 2 FC WM Fabp7 positive cells in NCI, MCI, and AD APOEε4 carriers and non-carriers. **A**–**L** Low magnification images of Fabp7 reactivity in the WM (dashed lines) of APOEε3 (**A**–**C**) and APOEε4 (**G**–**I**) carriers. Higher power images of WM Fabp7 immunoreactive cells in APOEε3 (**D**–**F**) and APOEε4 (**J**–**L**) carriers displaying a small, rounded, or oval-shaped morphology with thin processes like that seen in oligodendrocytes precursor cells in all clinical groups. Insets show higher power images of Fabp7 positive cells (arrows) in each panel. Scale bar in low magnification images I = 250 µm applies to panels (**A**–**C**, **G**–**I**). High power magnification images scale bar in L = 25 µm and inset = 10 µm applies to panels (**D**–**F**, **J**–**L**). **M** Quantification revealed a significant reduction in AD compared to NCI in APOEε4 non-carriers, that remained stable in carriers (NCI3/3 n = 10, MCI3/3 n = 11, AD3/3 n = 11, NCI3/4 n = 11, MCI3/4 n = 9, AD3/4 n = 11). Data shown in the bar graph is presented as mean ± SEM. Statistical significance was determined using the Kruskal–Wallis followed by a Dunn's test for comparisons across clinical groups and Mann–Whitney test for comparisons between carriers and non-carriers within each clinical group. Significance levels (*) were set at: *p < 0.05, **p < 0.01, ***p < 0.001. *GM* grey matter, *WM* white matter

co-localized with the ionized calcium-binding adaptor molecule 1 (Iba1), a well-established marker of microglia/macrophages (Fig. 3C, D, I, J), and with the oligodendrocyte marker oligodendrocytes transcription factor 2 (Olig2) (Fig. 3E, F, K, L) in both genotypes. Although ApoE-immunolabeled cells co-localized with Fabp7, a putative astrocyte marker, none of the latter co-localized with GFAP (Fig. 3M–T) [66] in the WM of both genotypes, suggesting a non-astrocyte phenotype.

FC Olig2-immunostaining in FC white matter in APOEε4 non-carriers and APOEε4 carriers during disease progression

We counted oligodendrocyte cell (Olig2 positive) number in the FC WM of APOEε4 carriers and APOEε4 non-carriers during the progression of AD. The number of Olig2 positive nuclei was significantly decreased in AD compared to NCI APOEε4 non-carriers (Fig. 4D–F, M, Table S1, Kruskal–Wallis followed by a Dunn's test: NCI > AD, p = 0.03). By contrast, no changes in the number of Olig2 positive nuclei were observed in APOEε4 carriers. However, a reduced number of Olig2-positive cells was observed only in MCI APOEε4 carriers compared to APOEε4 non-carriers (Fig. 4E, K, M, Table S1, Mann–Whitney test: MCI3/3 < MCI3/4, p = 0.02).

Quantitation of OD in MBP immunostaining and LFB histochemistry

We analyzed OD values of MBP and LFB, in FC WM of APOEε4 carriers and APOEε4 non-carriers during the progression of AD. The MBP antibody detects a protein that binds to the multilayered axonal membrane formed by oligodendrocytes, while LFB reflects lipids in the myelin of the WM (Fig. 5A–C). OD measurements of MBP revealed a significant increase in MCI compared to NCI and AD within the APOEε4 non-carrier group (Fig. 5D–F, P, Table S1, Kruskal–Wallis followed by a Dunn's test: MCI > NCI, AD, p = 0.002), which was not seen in

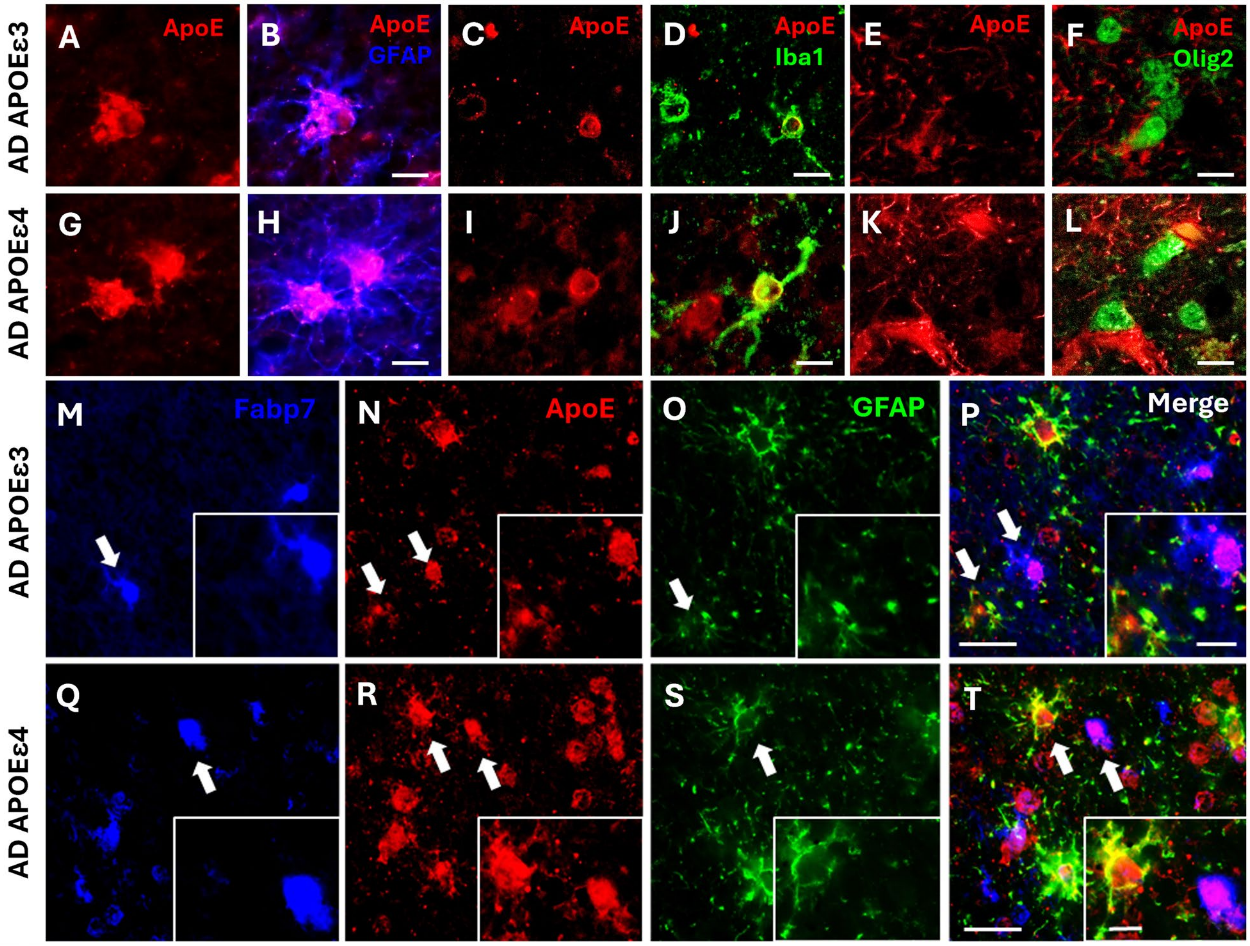

Fig. 3 FC WM ApoE and Fabp7 positive cells colocalize with different glial cell markers in AD carriers and non-carriers. Double-immunofluorescence images showing ApoE reactive cells (red) (**A**, **G**), (**C**, **I**), (**E**, **K**) that colocalize with the astrocytic glial fibrillar acidic protein (GFAP; blue) (**B**, **H**), the microglial ionized calcium-binding adaptor molecule 1 (Iba1; green) (**C**, **D**), and the oligodendrocyte marker, oligodendrocyte transcription factor 2 (Olig2; green) (**F**, **L**). Note that not all Iba1 and Olig2 positive cells express ApoE. Scale bar in A-L = 10 µM. Triple-immunofluorescent showing single Fabp7 (blue) (**M**–**Q**), ApoE (red) (**N**–**R**), GFAP (green) (**O**–**S**) cells and merged images (pink and yellow) (**P**, **T**). Insets show higher magnification images of Fabp7, ApoE and GFAP positive cells (white arrows). Note the consistent co-localization of GFAP and ApoE, while Fabp7 colocalizes only with ApoE. Scale bar in panel P, T = 25 µm and inset = 10 µm

APOEε4 carriers across clinical groups (Fig. 5G–I, P). A clinical group analysis revealed that MCI APOEε4 non-carriers presented greater MBP OD values than APOEε4 carriers (Fig. 5E, H, P. Table S1, Mann–Whitney test: MCI3/3 > MCI3/4, $p = 0.0008$).

OD values of LFB were significantly higher in MCI compared to NCI and AD in APOEε4 non-carriers (Fig. 5J–L, Q, Table S1, Kruskal–Wallis followed by a Dunn's test: MCI > NCI, AD, $p = 0.04$). However, there was a significant decrease in LFB OD values in AD compared to NCI among APOEε4 carriers (Fig. 5M–O, Q, Table S1, Kruskal–Wallis followed by a Dunn's test: NCI > AD, $p = 0.004$). NCI APOEε4 carriers had significantly greater LFB OD values compared to APOEε4 non-carriers (Fig. 5J, M, Q, Table S1, Mann–Whitney test: NCI3/3 > NCI3/4, $p = 0.01$). Although LFB histochemistry is an excellent marker to visualize myelin and lipid composition of myelin sheaths, it does not provide information related to myelin metabolism or the degree or type of lipidation in myelin. To answer this question, more advanced technologies would be required such as mass spectrometry.

Phosphorylated tau and plaque count in FC white and grey matter in APOEε4 non-carriers and APOEε4 carriers during disease progression

We evaluated the number of phosphorylated tau-positive cells (AT8) and APP/Aβ-positive plaques in both

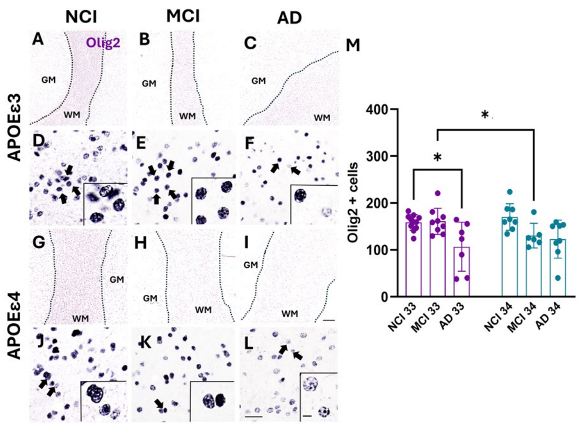

Fig. 4 FC WM Olig2 positive cells in NCI, MCI, and AD APOEε4 carriers and non-carriers. **A**–**L** Low magnification images of Olig2 (purple) reactivity in the WM (dashed lines) in APOEε3 (**A**–**C**) and APOEε4 (**G**–**I**) carriers. Higher power images of WM Olig2 immunoreactive cells in APOEε3 (**D**–**F**) and APOEε4 (**J**–**L**) WM displaying a small oval-shaped morphology in all clinical and genotype groups. Boxed insects show high power images of Olig2 positive cells in each panel (e.g., arrows in L). Scale bar in I = 250 µm and applies to panels **A**–**C**, **G**–**I**. Scale bar in L = 25 µm and inset = 10 µm applies to panels (**D**–**F**, **J**–**L**). **M** Quantification revealed a significant decrease in Olig2-positive nuclei in AD compared to NCI in APOEε4 non-carriers and in MCI carriers compared to non-carriers (NCI3/3 n = 11, MCI3/3 n = 10, AD3/3 n = 9, NCI3/4 n = 9, MCI3/4 n = 9, AD3/4 n = 9). Data shown in bar graph is presented as mean ± SEM. Statistical significance was determined using the Kruskal–Wallis followed by a Dunn's test for comparisons across clinical groups and Mann–Whitney test for comparisons between carriers and non-carriers within each clinical group. Significance levels (*) were set at: *p < 0.05, **p < 0.01, ***p < 0.001. *GM* grey matter, *WM* white matter

GM and WM of the FC. Qualitative analysis found that virtually all APP/Aβ lesions were diffuse plaques across clinical groups in the GM, except for a higher prevalence of neuritic plaques in AD APOEε4 carriers and APOEε4 non-carriers. By contrast, only a few plaques were seen in the WM. Quantitative analysis revealed no significant differences in APP/Aβ-positive plaque number in AD compared to MCI and NCI in APOEε4 non-carriers in WM. The qualitative evaluation of tau pathology in these cases found that AT8-positive cells were absent in 83% (25 of 30) of the cases examined, both in WM and GM. Although no tau pathology was observed in the GM of MCI APOEε4 carriers, statistical analysis revealed a significant increase in AT8-positive cells in the GM of AD compared to MCI in APOEε4 carriers (see Table S2, Kruskal–Wallis followed by Dunn's test: MCI < AD, p = 0.01). The increase in tau pathology is because of the remaining five cases four were in the AD APOEε4 carrier group.

Associations of cell counts and OD measurements with cognitive performance and neuropathological criteria

Applying linear regression models that included APOEε4 carrier status, we found a significant association between Olig2 cell counts and LFB OD (p < 0.001), but not MBP OD (p = 0.06) (see Table S3). We also performed a Spearman correlation analysis to assess whether the numbers of ApoE, Fabp7, and Olig2-positive cells, as well as OD measurements of MBP and LFB, were associated with each other (see Table S4) and/or with either cognitive performance or neuropathological criteria in both APOEε4 carriers and APOEε4 non-carriers (see Table S5). There was no statistical relationship between ApoE and Fabp7-positive cell numbers in WM, independent of genotype (Fig. 6A, B). Fabp7-positive cells correlated only with Olig2 in APOEε4 non-carriers (Fig. 6C, D, Spearman r = −0.58, p = 0.001). Regarding cognitive parameters, LFB OD measures positively correlated with global cognition in APOEε4 carriers but not in APOEε4 non-carriers (Fig. 6E, F, Spearman r = 0.55, p = 0.003). ApoE cell counts correlated with CERAD (Table S5, Spearman correlation r = 0.52, p = 0.003) and NIA-Reagan criteria (Table S5, Spearman correlation r = 0.58, p = 0.0007) but not Braak stage, while Fabp7 only positively correlated with CERAD in APOEε4 non-carriers (Table S5, Spearman correlation r = 0.56, p = 0.002).

Discussion

Although the ε4 allele of ApoE is linked to WM abnormalities, its effects on cell types related to myelination during the onset of AD are not well defined. The present immunohistochemical analysis revealed that the majority of cells containing cytoplasmic ApoE were astrocytes within the WM of the FC (area B10) [19]. By contrast, cytoplasmic ApoE immunostaining was observed to a lesser degree in other myelin related cell types, including microglia, oligodendrocytes and Fabp7-positive cells, which resembled OPCs in both genotypes [67]. We observed an increase in the number of WM ApoE-positive astrocytes in NCI and MCI in APOEε4 carriers compared to APOEε4 non-carriers, suggesting that an increase in ApoE protein accumulation in the cytoplasm of astrocytes is linked to the ε4 allele. A review of the literature failed to reveal studies linking ApoEε4-containing cell types or protein levels with ApoE allele status within the WM including the FC. A study revealed ApoE in vessel walls, astrocytes and oligodendrocytes and linked ApoE immunostaining to age-related WM abnormalities in humans [68]. In AD, ApoE-positive astrocytes have been reported to surround Aβ plaques in the temporal lobe and animal models indicate a crucial role in the deposition and accumulation of plaques. [32, 69, 70], suggesting a neuroinflammatory astrocytic response to this

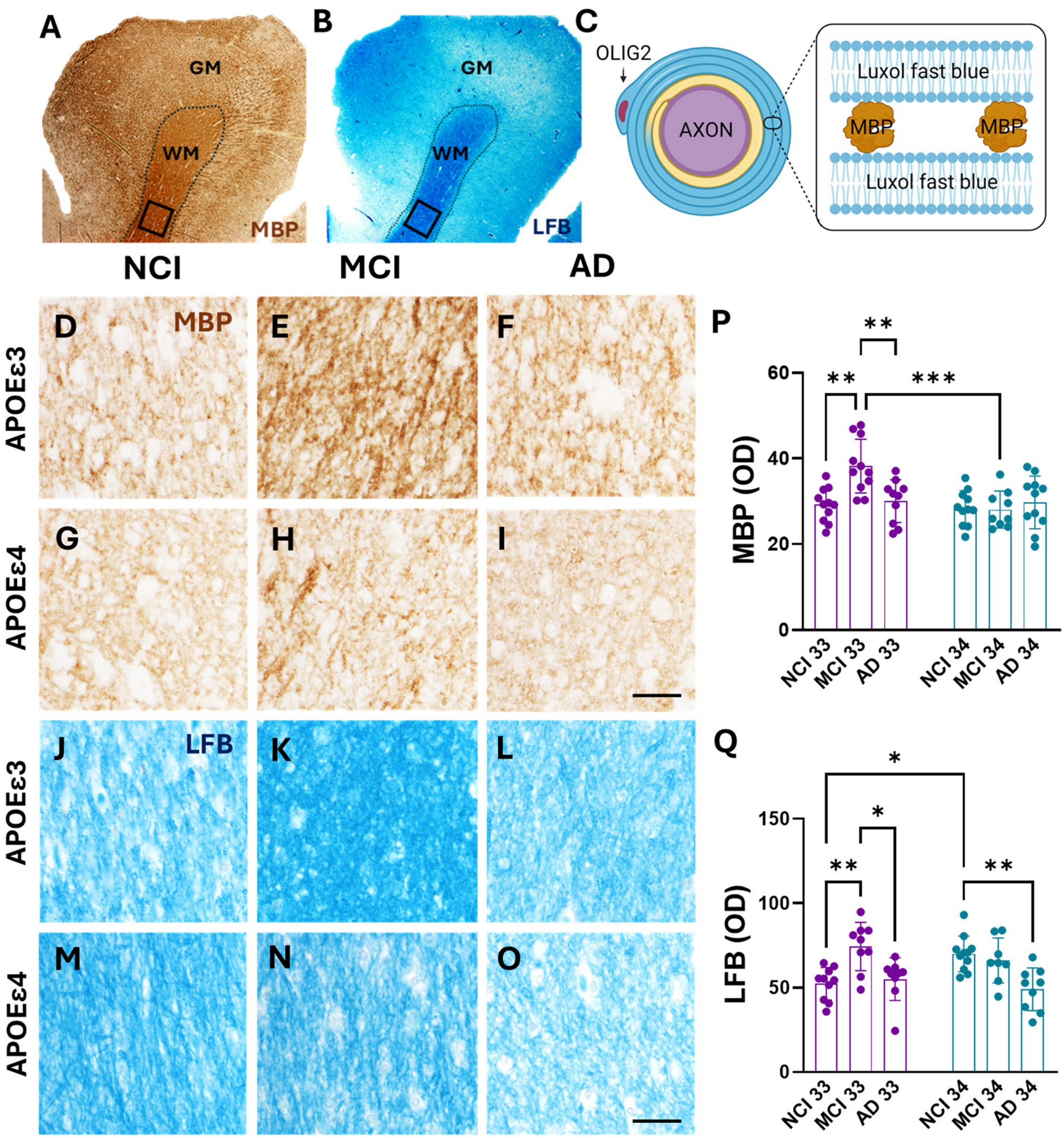

Fig. 5 FC WM MBP immunoreactive profiles and LFB histochemistry in NCI, MCI, and AD APOEε4 carriers and non-carriers. The low magnification images of myelin basic protein (MBP; brown) (**A**) and luxol fast blue (LFB) (**B**) staining showing the location of the WM (dashed lines) in the FC. **C** Schematic drawing showing the location of oligodendrocyte (Olig2), MBP and LFB during the formation of the myelin sheath (created with BioRender). Higher magnification images of MBP immunostaining (**D**–**I**) and LFB histochemistry (**J**–**O**) in APOEε3 and APOEε4 carriers. Note the increase in MBP reactivity in the MCI APOEε3 case (**E**), in LFB staining in NCI MCI non-carriers (**K**) and NCI APOEε4 carrier (**M**). Scale bar in I and O = 25 µm applies (**D**–**O**). (**P**) Statistical analysis revealed significantly higher OD measures of MBP in MCI compared to NCI and AD APOEε4 non-carriers (NCI3/3 n = 11, MCI3/3 n = 11, AD3/3 n = 10, NCI3/4 n = 11, MCI3/4 n = 9, AD3/4 n = 11). (**Q**) Quantitation of LFB revealed significantly greater levels in MCI non-carriers than NCI and AD non-carriers, while NCI carries showed higher levels than NCI non-carriers. (NCI3/3 n = 11, MCI3/3 n = 11, AD3/3 n = 10, NCI3/4 n = 11, MCI3/4 n = 9, AD3/4 n = 11). Data shown in bar graphs are presented as mean ± SEM. Statistical significance was determined by Kruskal–Wallis followed by a Dunn's test for comparisons across clinical groups and Mann–Whitney test for comparisons between carriers and non-carriers within each clinical group. Significance levels are indicated as follows: *p < 0.05, **p < 0.01, ***p < 0.001

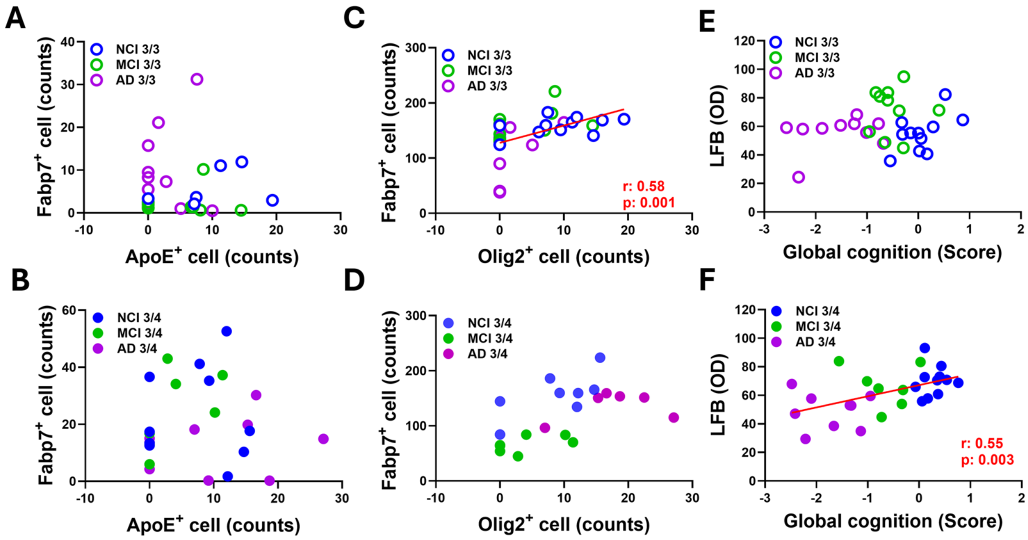

Fig. 6 Correlations between optical density, cell counts and cognitive variables. Linear regression graphs display correlations between Fabp7 and ApoE-positive cells in the WM for APOEε4 carriers (**A**) and APOEε4 non-carriers (**B**), between Fabp7 and Olig2-positive cells in APOEε4 carriers (**C**) and APOEε4 non-carriers (**D**) and between LFB optical density and global cognition scores in APOEε4 carriers (**E**) and APOEε4 non-carriers (**F**). Significant correlations were observed only between Fabp7 and Olig2 in APOEε4 non-carriers and LFB optical density and global cognition scores in APOEε4 carriers

protein. Alterations in astrocytic functionality, including impaired cholesterol accumulation and dysfunction in the secretion of the ApoE protein, occur when APOEε3 is converted to APOEε4 in iPSC-derived astrocytes [71, 72]. Perhaps, the functional consequences of these impairments interrupt the transport of astrocyte-derived lipids to oligodendrocytes altering axonal myelination [72] resulting in reduced axonal signal transmission [73], likely playing a role in impaired cognition. Here, we found that cognitive impairment was more pronounced in MCI and AD APOEε4 carriers compared to APOEε4 non-carriers (data not shown). This aligns with previous studies indicating greater cognitive decline and an earlier onset of symptoms in individuals carrying the ε4 allele [74].

Like ApoE, Fabp7 is an intracellular protein essential for fatty acid (FA) uptake, transport, metabolism, storage and its loss disrupt lipid homeostasis in the brain [75]. Compared to non-plaque brain regions, astrocytes surrounding Aβ plaques also exhibit increased Fabp7 staining in the cortical gray matter in AD [31]. Here, we observed that the number of Fabp7-positive cells in WM decreased in APOEε4 non-carriers during disease progression but remained stable in APOEε4 carriers. The lack of a reduction in Fabp7-positive cells in AD APOEε4 carriers compared to APOEε4 non-carriers requires further investigation, given the detrimental effects of the ε4 allele on myelination [29, 76]. One possible explanation for the preserved levels of this protein in APOEε4 carriers is that they require higher levels of FAs than non-carriers to maintain myelin integrity during disease progression. Fabp7 exhibits a strong affinity for docosahexaenoic acid (DHA), the predominant omega-3 polyunsaturated fatty acid (ω3-PUFA) in brain, while also binding with various FA derivatives, including endocannabinoids [77–79]. APOEε4 affects the metabolism of ω3-PUFAs, which are needed to control proinflammatory states [80], while transcriptomic analyses reported no effect of the ApoE genotype on Fabp7 transcript levels in iPSC cerebral organoids derived from AD patients [81]. The disconnect between these findings is likely related to the fact that organoids exist in an environment that does not reflect that found in the AD brain. Although Fabp7 is associated with an astrocytic inflammatory phenotype near Aβ plaques, we found no colocalization between Fabp7 and GFAP in the WM. However, we found a strong correlation between Olig2 and Fabp7-positive cell number among APOEε4 non-carriers. Interestingly, Fabp7 is also expressed in radial glia-like cells and oligodendrocyte precursor cells (OPC) [82, 83]. Since OPCs give rise to mature oligodendrocytes, which exhibit a morphology more like OPCs than to astrocytes [29], we suggest that WM Fabp7-positive cells are OPCs. However, the precise role(s) that Fabp7 and ApoE play in lipid processing and the development of AD pathology remains a major knowledge gap. Recent reports indicate that APOE risk variants in human induced iPS cell-derived microglia (iMG) induce cellular organelles containing lipid droplets (LDs), that are involved in lipid storage, energy regulation and lipid metabolism in microglia (i.e., lipid-droplet-accumulating microglia, LDAM), which are more prevalent in APOEε4/4 AD than control brain [84]. Although Fabp7 plays a key role in the formation and accumulation of LDs by accelerating the uptake and transport of fatty acids by regulating cellular lipid metabolism [31], its role in the formation of AD pathology remains unclear. However, treatment of primary hippocampal astrocyte cultures with Aβ fragment 25–35 (Aβ25–35) induces Fabp7 upregulation and increased expression in AD APP/PS1 transgenic mice [31]. An upregulation of Fabp7 produces an NF-κB-driven inflammatory response in induced astrocytes [85]. A recent study demonstrated that Fabp7 protects astrocytes from reactive oxygen species (ROS) toxicity through the formation of LDs suggesting a link between Fabp7, lipid homeostasis, and neurodegenerative disorders, including AD [85]. The role that Fabp7 and APOE play in the formation of LDs in AD requires continued investigation.

Here we report a decrease in Olig2 positive cells between groups within the APOEε4 non-carriers as described in both AD and animal models of this disease [72, 86, 87]. In the MCI APOEε4 carriers, the number of oligodendrocytes is lower than APOEε4 non-carriers, suggesting an early cellular demyelinating response associated with the ε4 allele. Following demyelination, OPCs differentiate, establish contacts with myelination-permissive axons and maintain myelin structure [88, 89]. Reports indicate that ApoE4 disrupts the maturation of OPCs into oligodendrocytes, which have been shown to be necessary for myelin sheath formation in hAPOE4 mice [72]. Interestingly, in patients with multiple sclerosis remyelination has been suggested to fail due to OPCs becoming quiescent and are not able to differentiate [90]. Perhaps similar effects occur in APOEε4 carriers because disrupted lipid transport from astrocytes to oligodendrocytes results in impaired differentiation and subsequent degeneration of oligodendrocytes.

With respect to myelin status, APOEε4 non-carriers displayed elevated levels of MBP and LFB in MCI compared to NCI and AD individuals, which coincided with stable numbers of oligodendrocytes. In contrast, upregulation of MBP was not observed in MCI APOEε4 carriers, indicating that the ε4 allele affects MBP production early in the disease process. Interestingly, viral-induced demyelination in mice trigger an upregulation of MBP mRNA synthesis following an inflammatory glial response [91], which does not occur in MCI APOEε4 carriers. We previously reported an increase in the number of WM astrocytes and microglia in MCI, suggesting an early inflammatory response during the preclinical stage of AD [65, 92]. Here, we suggest that an increase in MBP in APOEε4 non-carriers is an example of a putative compensatory response to early inflammation associated with the maintenance of myelin in the aged brain. In contrast, APOEε4 carriers may lack the ability to produce a similar MBP response needed to maintain myelin sheath integrity, including the production of lipids necessary for neurotransmission during the onset of AD [93] despite an increase in the number of WM astrocytes and microglia reported in the preclinical stage of AD [65, 92]. Additionally, the strong correlation between MBP levels and cognitive status in MCI and AD underscore the importance of increasing MBP levels to support cognitive function in the prodromal stage of AD in APOEε4 carriers [74].

Finally, APOEε4 carriers in the NCI group exhibited greater LFB staining but stable MBP levels, suggesting that the ε4 allele affects lipids involved in myelin metabolism in the non-demented aged brain [94, 95]. In addition, we found that LFB levels in APOEε4 carriers correlated with cognitive performance across clinical groups, suggesting that high myelin lipid levels preserve cognition, particularly in APOEε4ε4 allele carriers [96]. Perhaps maintaining lipid function has the potential to sustain cognition in advanced age even in the context of AD pathology [97].

A limitation of this study is its cross-sectional approach, which limits the ability to establish causal relationships between APOEε4, lipid transporters and myelin status over time. Therefore, performing longitudinal studies would provide a better understanding of the role that proteins related to myelination play in the onset of cognitive decline during the progression of AD. The AD cohort we examined lacked cases heterogeneous for APOEε4. It remains to be determined whether ε4/ε4 individuals would display greater WM lipid dysfunction compared to ε3/ε4 cases. A methodological caveat of this study is the inability to more accurately define the cell types labeled with ApoE in the WM during disease progression. Future co-staining experiments combined with more detailed quantitation are planned to address this issue. Although APOEε4 transgenic mice may be useful to evaluate some mechanistic questions based upon the present findings, the absence of an animal model that truly replicates prodromal AD hinders preclinical behavioral investigations. Although we are aware that data derived from human tissue clinical pathological investigations are correlative, the findings provided here are needed to develop novel animal models to investigate the role that APOEε4 plays in the pathobiology of WM dysfunction in AD. Future studies aimed at identifying specific lipids that change in the WM within other areas of the neo and limbic cortex, particularly the medial temporal lobe memory circuit as well as which glial cell types are most involved in lipid induced pathologies during disease progression in APOEε4 carriers versus APOEε4 non-carriers is warranted.

In summary, the number of WM ApoE-positive cells was greater in NCI and MCI, while Fabp7-positive cells increased only in AD. Olig2 cell counts and MBP immunostaining were lower in MCI APOEε4 carriers compared to APOEε4 non-carriers, while LFB levels were greater in NCI APOEε4 carriers compared to APOEε4 non-carriers. Correlational analysis revealed no association between ApoE and Fabp7-positive cells, whereas LFB values were positively correlated with global cognitive performance in APOEε4 carriers across clinical groups. Overall, our findings suggest that the APOEε4 allele compromises myelin by disrupting ApoE and Fabp7, key lipid transporters, which play a role in the maintenance of myelination in the WM, at least in the FC during the onset of AD. The present finding suggests that targeting myelin lipid metabolism is a potential therapeutic strategy for managing cognitive impairment early in AD, particularly in APOEε4 carriers.

Abbreviations

AD	Alzheimer's disease
ApoE	Apolipoprotein E
APOEε4	ApoE ε4 allele
Aβ	Amyloid-β
CERAD	Consortium to Establish a Registry for Alzheimer's disease
DAB	3,3′-Diaminobenzidine tetrahydrochloride
FAs	Fatty acids
Fabp7	Fatty acid-binding protein 7
FC	Frontal cortex
GFAP	Glial fibrillary acidic protein
Iba1	Ionized calcium-binding adaptor molecule 1
LFB	Luxol fast blue
MBP	Myelin basic protein
MCI	Mild cognitive impairment
MRI	Magnetic resonance imaging
NCI	No cognitive impairment
OD	Optical density
Olig2	Oligodendrocyte transcription factor 2
OPC	Oligodendrocyte precursor cells
PMI	Postmortem interval
ROI	Region of interest
TDP-43	Transactive response DNA-binding protein 43
WB	Western blot
WM	White matter
ω3-PUFAs	Omega-3 polyunsaturated fatty acids

Supplementary Information

The online version contains supplementary material available at https://doi.org/10.1186/s12974-025-03349-y.

Supplementary material 1: Table S1. Count Data and Optical Density Stratified by Clinical Group and APOEε4 Status. Table S2. Correlation Values for Optical Density and Count Data. Table S3. Correlation Values for Optical Density and Count Data with Cognitive and Neuropathological Variables.

Acknowledgements
We are indebted to the nuns, priests, and lay brothers who participated in the Rush Religious Orders Study, without whom this work would not be possible, and to the members of the Rush ADC.

Author contributions
S.P, E.M and M.M.R. designed, conceptualized and wrote the manuscript. M.M.R performed immunohistochemical experiments and data quantification. M. M. H. performed the statistical analysis.

Funding
This study was supported by Grants PO1AG014449, RO1AG043375, P30AG010161 and P30AG042146, and RF1AG081286 from the National Institute on Aging, Barrow Neurological Institute and Arizona Alzheimer's Consortium.

Availability of data and materials
No datasets were generated or analysed during the current study.

Declarations

Ethics approval and consent to participate
The Human Research Committees of Rush University Medical Center and Dignity Health approved this study and written informed consent for research and brain autopsy was obtained from the participants or their family/guardians.

Consent for publication
Not applicable.

Competing interests
The authors declare no competing interests.

Received: 26 September 2024 Accepted: 15 January 2025
Published online: 30 January 2025

References

1. Arai H, Yamamoto A, Matsuzawa Y, Saito Y, Yamada N, Oikawa S, Mabuchi H, Teramoto T, Sasaki J, Nakaya N, et al. Polymorphisms of apolipoprotein e and methylenetetrahydrofolate reductase in the Japanese population. J Atheroscler Thromb. 2007;14(4):167–71.
2. Zhong Z, Wu H, Wu H, Zhao P. Analysis of apolipoprotein E genetic polymorphism in a large ethnic Hakka population in southern China. Genet Mol Biol. 2018;41(4):742–9.
3. Fuzikawa AK, Peixoto SV, Taufer M, Moriguchi EH, Lima-Costa MF. Apolipoprotein E polymorphism distribution in an elderly Brazilian population: the Bambui Health and Aging Study. Braz J Med Biol Res. 2007;40(11):1429–34.
4. Benyahya F, Barakat A, Ghailani N, Bennani M. Apolipoprotein E polymorphism in the population of northern Morocco: frequency and effect on lipid parameters. Pan Afr Med J. 2013;15:157.
5. Fortea J, Pegueroles J, Alcolea D, Belbin O, Dols-Icardo O, Vaque-Alcazar L, Videla L, Gispert JD, Suarez-Calvet M, Johnson SC, et al. APOE4 homozygozity represents a distinct genetic form of Alzheimer's disease. Nat Med. 2024. https://doi.org/10.1038/s41591-024-03127-y.
6. Raulin AC, Doss SV, Trottier ZA, Ikezu TC, Bu G, Liu CC. ApoE in Alzheimer's disease: pathophysiology and therapeutic strategies. Mol Neurodegener. 2022;17(1):72.
7. Yamazaki Y, Zhao N, Caulfield TR, Liu CC, Bu G. Apolipoprotein E and Alzheimer disease: pathobiology and targeting strategies. Nat Rev Neurol. 2019;15(9):501–18.
8. Rosenberg JB, Kaplitt MG, De BP, Chen A, Flagiello T, Salami C, Pey E, Zhao L, Ricart Arbona RJ, Monette S, et al. AAVrh.10-mediated APOE2 central nervous system gene therapy for APOE4-associated Alzheimer's disease. Hum Gene Ther Clin Dev. 2018;29(1):24–47.

9. Ponomareva NV, Korovaitseva GI, Rogaev EI. EEG alterations in non-demented individuals related to apolipoprotein E genotype and to risk of Alzheimer disease. Neurobiol Aging. 2008;29(6):819–27.
10. Schmechel DE, Saunders AM, Strittmatter WJ, Crain BJ, Hulette CM, Joo SH, Pericak-Vance MA, Goldgaber D, Roses AD. Increased amyloid beta-peptide deposition in cerebral cortex as a consequence of apolipoprotein E genotype in late-onset Alzheimer disease. Proc Natl Acad Sci U S A. 1993;90(20):9649–53.
11. Koutsodendris N, Nelson MR, Rao A, Huang Y. Apolipoprotein E and Alzheimer's disease: findings, hypotheses, and potential mechanisms. Annu Rev Pathol. 2022;17:73–99.
12. Bu G. Apolipoprotein E and its receptors in Alzheimer's disease: pathways, pathogenesis and therapy. Nat Rev Neurosci. 2009;10(5):333–44.
13. Mishra S, Blazey TM, Holtzman DM, Cruchaga C, Su Y, Morris JC, Benzinger TLS, Gordon BA. Longitudinal brain imaging in preclinical Alzheimer disease: impact of APOE epsilon4 genotype. Brain. 2018;141(6):1828–39.
14. Toledo JB, Habes M, Sotiras A, Bjerke M, Fan Y, Weiner MW, Shaw LM, Davatzikos C, Trojanowski JQ, Alzheimer's Disease Neuroimaging I. APOE effect on amyloid-beta PET spatial distribution, deposition rate, and cut-points. J Alzheimers Dis. 2019;69(3):783–93.
15. Novy MJ, Newbury SF, Liemisa B, Morales-Corraliza J, Alldred MJ, Ginsberg SD, Mathews PM. Expression and proteolytic processing of the amyloid precursor protein is unaffected by the expression of the three human apolipoprotein E alleles in the brains of mice. Neurobiol Aging. 2022;110:73–6.
16. Montagne A, Nikolakopoulou AM, Huuskonen MT, Sagare AP, Lawson EJ, Lazic D, Rege SV, Grond A, Zuniga E, Barnes SR, et al. APOE4 accelerates advanced-stage vascular and neurodegenerative disorder in old Alzheimer's mice via cyclophilin A independently of amyloid-beta. Nat Aging. 2021;1(6):506–20.
17. Zhu Y, Nwabuisi-Heath E, Dumanis SB, Tai LM, Yu C, Rebeck GW, LaDu MJ. APOE genotype alters glial activation and loss of synaptic markers in mice. Glia. 2012;60(4):559–69.
18. Fernandez CG, Hamby ME, McReynolds ML, Ray WJ. The role of APOE4 in disrupting the homeostatic functions of astrocytes and microglia in aging and Alzheimer's disease. Front Aging Neurosci. 2019;11:14.
19. Boyles JK, Pitas RE, Wilson E, Mahley RW, Taylor JM. Apolipoprotein E associated with astrocytic glia of the central nervous system and with nonmyelinating glia of the peripheral nervous system. J Clin Invest. 1985;76(4):1501–13.
20. Aoki K, Uchihara T, Sanjo N, Nakamura A, Ikeda K, Tsuchiya K, Wakayama Y. Increased expression of neuronal apolipoprotein E in human brain with cerebral infarction. Stroke. 2003;34(4):875–80.
21. Grubman A, Chew G, Ouyang JF, Sun G, Choo XY, McLean C, Simmons RK, Buckberry S, Vargas-Landin DB, Poppe D, et al. A single-cell atlas of entorhinal cortex from individuals with Alzheimer's disease reveals cell-type-specific gene expression regulation. Nat Neurosci. 2019;22(12):2087–97.
22. Gomez-Ramos P, Mufson EJ, Moran MA. Apolipoprotein E immunoreactivity in neurons and neurofibrillary degeneration of aged non-demented and Alzheimer's disease patients. Microsc Res Tech. 2001;55(1):48–58.
23. Camargo N, Goudriaan A, van Deijk AF, Otte WM, Brouwers JF, Lodder H, Gutmann DH, Nave KA, Dijkhuizen RM, Mansvelder HD, et al. Oligodendroglial myelination requires astrocyte-derived lipids. PLoS Biol. 2017;15(5):e1002605.
24. Molina-Gonzalez I, Holloway RK, Jiwaji Z, Dando O, Kent SA, Emelianova K, Lloyd AF, Forbes LH, Mahmood A, Skripuletz T, et al. Astrocyte-oligodendrocyte interaction regulates central nervous system regeneration. Nat Commun. 2023;14(1):3372.
25. Dimas P, Montani L, Pereira JA, Moreno D, Trotzmuller M, Gerber J, Semenkovich CF, Kofeler HC, Suter U. CNS myelination and remyelination depend on fatty acid synthesis by oligodendrocytes. Elife. 2019;8:e44702.
26. Chrast R, Saher G, Nave KA, Verheijen MH. Lipid metabolism in myelinating glial cells: lessons from human inherited disorders and mouse models. J Lipid Res. 2011;52(3):419–34.
27. Cantuti-Castelvetri L, Fitzner D, Bosch-Queralt M, Weil MT, Su M, Sen P, Ruhwedel T, Mitkovski M, Trendelenburg G, Lutjohann D, et al. Defective cholesterol clearance limits remyelination in the aged central nervous system. Science. 2018;359(6376):684–8.
28. Safaiyan S, Besson-Girard S, Kaya T, Cantuti-Castelvetri L, Liu L, Ji H, Schifferer M, Gouna G, Usifo F, Kannaiyan N, et al. White matter aging drives microglial diversity. Neuron. 2021;109(7):1100–17.
29. Foerster S, de Fuente AG, Kagawa Y, Bartels T, Owada Y, Franklin RJM. The fatty acid binding protein FABP7 is required for optimal oligodendrocyte differentiation during myelination but not during remyelination. Glia. 2020;68(7):1410–20.
30. Killoy KM, Harlan BA, Pehar M, Vargas MR. FABP7 upregulation induces a neurotoxic phenotype in astrocytes. Glia. 2020;68(12):2693–704.
31. Hamilton HL, Kinscherf NA, Balmer G, Bresque M, Salamat SM, Vargas MR, Pehar M. FABP7 drives an inflammatory response in human astrocytes and is upregulated in Alzheimer's disease. Geroscience. 2024;46(2):1607–25.
32. Mahan TE, Wang C, Bao X, Choudhury A, Ulrich JD, Holtzman DM. Selective reduction of astrocyte apoE3 and apoE4 strongly reduces Abeta accumulation and plaque-related pathology in a mouse model of amyloidosis. Mol Neurodegener. 2022;17(1):13.
33. Bartzokis G. Age-related myelin breakdown: a developmental model of cognitive decline and Alzheimer's disease. Neurobiol Aging. 2004;25(1):5–18.
34. Amlien IK, Fjell AM. Diffusion tensor imaging of white matter degeneration in Alzheimer's disease and mild cognitive impairment. Neuroscience. 2014;276:206–15.
35. O'Dwyer L, Lamberton F, Bokde AL, Ewers M, Faluyi YO, Tanner C, Mazoyer B, O'Neill D, Bartley M, Collins DR, et al. Using diffusion tensor imaging and mixed-effects models to investigate primary and secondary white matter degeneration in Alzheimer's disease and mild cognitive impairment. J Alzheimers Dis. 2011;26(4):667–82.
36. Cavedo E, Lista S, Rojkova K, Chiesa PA, Houot M, Brueggen K, Blautzik J, Bokde ALW, Dubois B, Barkhof F, et al. Disrupted white matter structural networks in healthy older adult APOE epsilon4 carriers - an international multicenter DTI study. Neuroscience. 2017;357:119–33.
37. Operto G, Cacciaglia R, Grau-Rivera O, Falcon C, Brugulat-Serrat A, Rodenas P, Ramos R, Moran S, Esteller M, Bargallo N, et al. White matter microstructure is altered in cognitively normal middle-aged APOE-epsilon4 homozygotes. Alzheimers Res Ther. 2018;10(1):48.
38. Lacey C, Paterson T, Gawryluk JR, Alzheimer's Disease Neuroimaging I. Impact of APOE-epsilon alleles on brain structure and cognitive function in healthy older adults: a VBM and DTI replication study. PLoS ONE. 2024;19(4):e0292576.
39. Smith JC, Lancaster MA, Nielson KA, Woodard JL, Seidenberg M, Durgerian S, Sakaie K, Rao SM. Interactive effects of physical activity and APOE-epsilon4 on white matter tract diffusivity in healthy elders. Neuroimage. 2016;131:102–12.
40. Blanchard JW, Akay LA, Davila-Velderrain J, von Maydell D, Mathys H, Davidson SM, Effenberger A, Chen CY, Maner-Smith K, Hajjar I, et al. APOE4 impairs myelination via cholesterol dysregulation in oligodendrocytes. Nature. 2022;611(7937):769–79.
41. Cheng GW, Mok KK, Yeung SH, Kofler J, Herrup K, Tse KH. Apolipoprotein E epsilon4 mediates myelin breakdown by targeting oligodendrocytes in sporadic Alzheimer disease. J Neuropathol Exp Neurol. 2022;81(9):717–30.
42. Sock E, Wegner M. Transcriptional control of myelination and remyelination. Glia. 2019;67(11):2153–65.
43. Herbert AL, Monk KR. Advances in myelinating glial cell development. Curr Opin Neurobiol. 2017;42:53–60.
44. Malek-Ahmadi M, Perez SE, Chen K, Mufson EJ. Neuritic and diffuse plaque associations with memory in non-cognitively impaired elderly. J Alzheimers Dis. 2016;53(4):1641–52.
45. Mufson EJ, Malek-Ahmadi M, Snyder N, Ausdemore J, Chen K, Perez SE. Braak stage and trajectory of cognitive decline in noncognitively impaired elders. Neurobiol Aging. 2016;43:101–10.
46. Malek-Ahmadi M, Chen K, Perez SE, He A, Mufson EJ. Cognitive composite score association with Alzheimer's disease plaque and tangle pathology. Alzheimers Res Ther. 2018;10(1):90.
47. Price JL, McKeel DW Jr, Buckles VD, Roe CM, Xiong C, Grundman M, Hansen LA, Petersen RC, Parisi JE, Dickson DW, et al. Neuropathology of nondemented aging: presumptive evidence for preclinical Alzheimer disease. Neurobiol Aging. 2009;30(7):1026–36.
48. Scholl M, Lockhart SN, Schonhaut DR, O'Neil JP, Janabi M, Ossenkoppele R, Baker SL, Vogel JW, Faria J, Schwimmer HD, et al. PET imaging of Tau deposition in the aging human brain. Neuron. 2016;89(5):971–82.

49. Perez SE, Getova DP, He B, Counts SE, Geula C, Desire L, Coutadeur S, Peillon H, Ginsberg SD, Mufson EJ. Rac1b increases with progressive tau pathology within cholinergic nucleus basalis neurons in Alzheimer's disease. Am J Pathol. 2012;180(2):526–40.
50. Davis DG, Schmitt FA, Wekstein DR, Markesbery WR. Alzheimer neuropathologic alterations in aged cognitively normal subjects. J Neuropathol Exp Neurol. 1999;58(4):376–88.
51. Bennett DA, Schneider JA, Bienias JL, Evans DA, Wilson RS. Mild cognitive impairment is related to Alzheimer disease pathology and cerebral infarctions. Neurology. 2005;64(5):834–41.
52. Mufson EJ, Chen EY, Cochran EJ, Beckett LA, Bennett DA, Kordower JH. Entorhinal cortex beta-amyloid load in individuals with mild cognitive impairment. Exp Neurol. 1999;158(2):469–90.
53. McKhann G, Drachman D, Folstein M, Katzman R, Price D, Stadlan EM. Clinical diagnosis of Alzheimer's disease: report of the NINCDS-ADRDA work group under the auspices of department of health and human services task force on Alzheimer's disease. Neurology. 1984;34(7):939–44.
54. Rubin EH, Morris JC, Grant EA, Vendegna T. Very mild senile dementia of the Alzheimer type. I. Clinical assessment. Arch Neurol. 1989;46(4):379–82.
55. Petersen RC, Smith GE, Ivnik RJ, Tangalos EG, Schaid DJ, Thibodeau SN, Kokmen E, Waring SC, Kurland LT. Apolipoprotein E status as a predictor of the development of Alzheimer's disease in memory-impaired individuals. JAMA. 1995;273(16):1274–8.
56. Ebly EM, Hogan DB, Parhad IM. Cognitive impairment in the nondemented elderly. Results from the Canadian Study of Health and Aging. Arch Neurol. 1995;52(6):612–9.
57. Devanand DP, Folz M, Gorlyn M, Moeller JR, Stern Y. Questionable dementia: clinical course and predictors of outcome. J Am Geriatr Soc. 1997;45(3):321–8.
58. Albert M, Smith LA, Scherr PA, Taylor JO, Evans DA, Funkenstein HH. Use of brief cognitive tests to identify individuals in the community with clinically diagnosed Alzheimer's disease. Int J Neurosci. 1991;57(3–4):167–78.
59. Flicker C, Ferris SH, Reisberg B. Mild cognitive impairment in the elderly: predictors of dementia. Neurology. 1991;41(7):1006–9.
60. Schmitt FA, Nelson PT, Abner E, Scheff S, Jicha GA, Smith C, Cooper G, Mendiondo M, Danner DD, Van Eldik LJ, et al. University of Kentucky Sanders-Brown healthy brain aging volunteers: donor characteristics, procedures and neuropathology. Curr Alzheimer Res. 2012;9(6):724–33.
61. Braak H, Braak E. Neuropathological stageing of Alzheimer-related changes. Acta Neuropathol. 1991;82(4):239–59.
62. Newell KL, Hyman BT, Growdon JH, Hedley-Whyte ET. Application of the National Institute on Aging (NIA)-Reagan Institute criteria for the neuropathological diagnosis of Alzheimer disease. J Neuropathol Exp Neurol. 1999;58(11):1147–55.
63. Mirra SS. The CERAD neuropathology protocol and consensus recommendations for the postmortem diagnosis of Alzheimer's disease: a commentary. Neurobiol Aging. 1997;18(4 Suppl):S91-94.
64. Hyman BT, Phelps CH, Beach TG, Bigio EH, Cairns NJ, Carrillo MC, Dickson DW, Duyckaerts C, Frosch MP, Masliah E, et al. National Institute on Aging-Alzheimer's Association guidelines for the neuropathologic assessment of Alzheimer's disease. Alzheimers Dement. 2012;8(1):1–13.
65. Moreno-Rodriguez M, Perez SE, Nadeem M, Malek-Ahmadi M, Mufson EJ. Frontal cortex chitinase and pentraxin neuroinflammatory alterations during the progression of Alzheimer's disease. J Neuroinflammation. 2020;17(1):58.
66. Huang H, He W, Tang T, Qiu M. Immunological markers for central nervous system glia. Neurosci Bull. 2023;39(3):379–92.
67. Sampaio-Baptista C, Johansen-Berg H. White matter plasticity in the adult brain. Neuron. 2017;96(6):1239–51.
68. Schmidt R, Schmidt H, Haybaeck J, Loitfelder M, Weis S, Cavalieri M, Seiler S, Enzinger C, Ropele S, Erkinjuntti T, et al. Heterogeneity in age-related white matter changes. Acta Neuropathol. 2011;122(2):171–85.
69. Koistinaho M, Lin S, Wu X, Esterman M, Koger D, Hanson J, Higgs R, Liu F, Malkani S, Bales KR, et al. Apolipoprotein E promotes astrocyte colocalization and degradation of deposited amyloid-beta peptides. Nat Med. 2004;10(7):719–26.
70. Thangavel R, Bhagavan SM, Ramaswamy SB, Surpur S, Govindarajan R, Kempuraj D, Zaheer S, Raikwar S, Ahmed ME, Selvakumar GP, et al. Co-expression of glia maturation factor and apolipoprotein E4 in Alzheimer's disease brain. J Alzheimers Dis. 2018;61(2):553–60.
71. Lin YT, Seo J, Gao F, Feldman HM, Wen HL, Penney J, Cam HP, Gjoneska E, Raja WK, Cheng J, et al. APOE4 causes widespread molecular and cellular alterations associated with Alzheimer's disease phenotypes in human iPSC-derived brain cell types. Neuron. 2018;98(6):1141–54.
72. Mok KK, Yeung SH, Cheng GW, Ma IW, Lee RH, Herrup K, Tse KH. Apolipoprotein E epsilon4 disrupts oligodendrocyte differentiation by interfering with astrocyte-derived lipid transport. J Neurochem. 2023;165(1):55–75.
73. Monje M. Myelin plasticity and nervous system function. Annu Rev Neurosci. 2018;41:61–76.
74. Polsinelli AJ, Logan PE, Lane KA, Manchella MK, Nemes S, Sanjay AB, Gao S, Apostolova LG. APOE epsilon4 carrier status and sex differentiate rates of cognitive decline in early- and late-onset Alzheimer's disease. Alzheimers Dement. 2023;19(5):1983–93.
75. Owada Y, Abdelwahab SA, Kitanaka N, Sakagami H, Takano H, Sugitani Y, Sugawara M, Kawashima H, Kiso Y, Mobarakeh JI, et al. Altered emotional behavioral responses in mice lacking brain-type fatty acid-binding protein gene. Eur J Neurosci. 2006;24(1):175–87.
76. Sharifi K, Ebrahimi M, Kagawa Y, Islam A, Tuerxun T, Yasumoto Y, Hara T, Yamamoto Y, Miyazaki H, Tokuda N, et al. Differential expression and regulatory roles of FABP5 and FABP7 in oligodendrocyte lineage cells. Cell Tissue Res. 2013;354(3):683–95.
77. Balendiran GK, Schnutgen F, Scapin G, Borchers T, Xhong N, Lim K, Godbout R, Spener F, Sacchettini JC. Crystal structure and thermodynamic analysis of human brain fatty acid-binding protein. J Biol Chem. 2000;275(35):27045–54.
78. Kaczocha M, Glaser ST, Deutsch DG. Identification of intracellular carriers for the endocannabinoid anandamide. Proc Natl Acad Sci U S A. 2009;106(15):6375–80.
79. Xu LZ, Sanchez R, Sali A, Heintz N. Ligand specificity of brain lipid-binding protein. J Biol Chem. 1996;271(40):24711–9.
80. Tomaszewski N, He X, Solomon V, Lee M, Mack WJ, Quinn JF, Braskie MN, Yassine HN. Effect of APOE genotype on plasma docosahexaenoic acid (DHA), eicosapentaenoic acid, arachidonic acid, and hippocampal volume in the Alzheimer's disease cooperative study-sponsored DHA clinical trial. J Alzheimers Dis. 2020;74(3):975–90.
81. Zhao J, Fu Y, Yamazaki Y, Ren Y, Davis MD, Liu CC, Lu W, Wang X, Chen K, Cherukuri Y, et al. APOE4 exacerbates synapse loss and neurodegeneration in Alzheimer's disease patient iPSC-derived cerebral organoids. Nat Commun. 2020;11(1):5540.
82. Sharifi K, Morihiro Y, Maekawa M, Yasumoto Y, Hoshi H, Adachi Y, Sawada T, Tokuda N, Kondo H, Yoshikawa T, et al. FABP7 expression in normal and stab-injured brain cortex and its role in astrocyte proliferation. Histochem Cell Biol. 2011;136(5):501–13.
83. Kurtz A, Zimmer A, Schnutgen F, Bruning G, Spener F, Muller T. The expression pattern of a novel gene encoding brain-fatty acid binding protein correlates with neuronal and glial cell development. Development. 1994;120(9):2637–49.
84. Marschallinger J, Iram T, Zardeneta M, Lee SE, Lehallier B, Haney MS, Pluvinage JV, Mathur V, Hahn O, Morgens DW, et al. Lipid-droplet-accumulating microglia represent a dysfunctional and proinflammatory state in the aging brain. Nat Neurosci. 2020;23(2):194–208.
85. Islam A, Kagawa Y, Miyazaki H, Shil SK, Umaru BA, Yasumoto Y, Yamamoto Y, Owada Y. FABP7 protects astrocytes against ROS toxicity via lipid droplet formation. Mol Neurobiol. 2019;56(8):5763–79.
86. Qiu D, Zhou S, Donnelly J, Xia D, Zhao L. Aerobic exercise attenuates abnormal myelination and oligodendrocyte differentiation in 3xTg-AD mice. Exp Gerontol. 2023;182:112293.
87. Chacon-De-La-Rocha I, Fryatt G, Rivera AD, Verkhratsky A, Raineteau O, Gomez-Nicola D, Butt AM. Accelerated dystrophy and decay of oligodendrocyte precursor cells in the APP/PS1 model of Alzheimer's-like pathology. Front Cell Neurosci. 2020;14:575082.
88. Levine JM, Reynolds R. Activation and proliferation of endogenous oligodendrocyte precursor cells during ethidium bromide-induced demyelination. Exp Neurol. 1999;160(2):333–47.
89. Kang SH, Fukaya M, Yang JK, Rothstein JD, Bergles DE. NG2+ CNS glial progenitors remain committed to the oligodendrocyte lineage in postnatal life and following neurodegeneration. Neuron. 2010;68(4):668–81.
90. Cunniffe N, Coles A. Promoting remyelination in multiple sclerosis. J Neurol. 2021;268(1):30–44.

91. Kristensson K, Holmes KV, Duchala CS, Zeller NK, Lazzarini RA, Dubois-Dalcq M. Increased levels of myelin basic protein transcripts in virus-induced demyelination. Nature. 1986;322(6079):544–7.
92. Jacobs HI, Clerx L, Gronenschild EH, Aalten P, Verhey FR. White matter hyperintensities are positively associated with cortical thickness in Alzheimer's disease. J Alzheimers Dis. 2014;39(2):409–22.
93. Tognatta R, Karl MT, Fyffe-Maricich SL, Popratiloff A, Garrison ED, Schenck JK, Abu-Rub M, Miller RH. Astrocytes are required for oligodendrocyte survival and maintenance of myelin compaction and integrity. Front Cell Neurosci. 2020;14:74.
94. Barnes-Velez JA, Aksoy Yasar FB, Hu J. Myelin lipid metabolism and its role in myelination and myelin maintenance. Innovation (Camb). 2023;4(1):100360.
95. Moreno-Rodriguez M, Perez SE, Martinez-Gardeazabal J, Manuel I, Malek-Ahmadi M, Rodriguez-Puertas R, Mufson EJ. Frontal cortex lipid alterations during the onset of Alzheimer's disease. J Alzheimers Dis. 2024;98(4):1515–32.
96. Poitelon Y, Kopec AM, Belin S. Myelin fat facts: an overview of lipids and fatty acid metabolism. Cells. 2020;9(4):812.
97. Montine TJ, Cholerton BA, Corrada MM, Edland SD, Flanagan ME, Hemmy LS, Kawas CH, White LR. Concepts for brain aging: resistance, resilience, reserve, and compensation. Alzheimers Res Ther. 2019;11(1):22.

Publisher's Note